Caldesmon Binding to Actin Is Regulated by Calmodulin and Phosphorylation via Different Mechanisms†

Renjian Huang,‡ Liansheng Li,‡ Hongqiu Guo, and C.-L. Albert Wang*

Muscle and Motility Group, Boston Biomedical Research Institute, 64 Grove Street, Watertown, Massachusetts 02472

Received September 16, 2002; Revised Manuscript Received January 11, 2003

ABSTRACT: Smooth muscle caldesmon (CaD) binds F-actin and inhibits actomyosin ATPase activity. The inhibition is reversed by Ca^{2+}/calmodulin (CaM). CaD is also phosphorylated upon stimulation at sites specific for mitogen-activated protein kinases (MAPKs). Because of these properties, CaD is thought to be involved in the regulation of smooth muscle contraction. The molecular mechanism of the reversal of inhibition is not well understood. We have expressed His_6-tagged fragments containing the sequence of the C-terminal region of human (from M563 to V793) and chicken (from M563 to P771) CaD as well as a variant of the chicken isoform with a Q766C point mutation. By cleavages with proteases, followed by high-speed cosedimentation with F-actin and mass spectrometry, we found that within the C-terminal region of CaD there are multiple actin contact points forming two clusters. Intramolecular fluorescence resonance energy transfer between probes attached to cysteine residues (the endogenous C595 and the engineered C766) located in these two clusters revealed that the C-terminal region of CaD is elongated, but it becomes more compact when bound to actin. Binding of CaM restores the elongated conformation and facilitates dissociation of the C-terminal CaD fragment from F-actin. When the CaD fragment was phosphorylated with a MAPK, only one of the two actin-binding clusters dissociated from F-actin, whereas the other remained bound. Taken together, these results demonstrate that while both Ca^{2+}/CaM and MAPK phosphorylation govern CaD's function via a conformational change, the regulatory mechanisms are different.

Smooth muscle contraction controls a wide range of vital physiological functions. Its proper regulation is essential for the normal operation of the human body. While smooth muscles are usually stimulated by an increase in the intracellular calcium level, they do contract in a Ca^{2+}-independent manner under some conditions. Understanding how smooth muscle contraction is regulated under a variety of different conditions is thus very important. The primary mechanism of smooth muscle regulation relies on the level of myosin activation, which involves myosin light chain kinase and myosin phosphatase. Whether additional regulatory proteins exist that may act via the actin filament to enhance the versatility of smooth muscle contractility is a possibility that remains to be tested.

Caldesmon (CaD)[1] is a major actin-binding protein in smooth muscle cells. Binding of CaD to F-actin in vitro inhibits the weak type of interaction between actin and myosin, and thereby attenuates the actomyosin ATPase activity (*1*, *2*). Such inhibition is likely due to a partial overlap on the actin surface between the myosin motor domain and the C-terminal region of CaD, where the well-established (*3*−*7*) actin-binding sites are located. It is also generally believed that through actin binding CaD plays an inhibitory role in vivo, providing a fine-tuning of the contractile force in the diverse smooth muscle activities.

Binding of CaD to actin (*8*) and the inhibition of the actomyosin ATPase activity (*2*) are reversed by calmodulin (CaM) in the presence of Ca^{2+}. This property suggests a regulatory mechanism for CaD's inhibitory function (*9*, *10*). However, whether Ca^{2+}/CaM regulates CaD in vivo remains a point of debate, mainly because of the moderate affinity (10^6−10^7 M^{-1}) between CaM and CaD (*9*, *11*−*13*), which would require a relatively high intracellular concentration of free CaM. By using a fluorescently labeled CaD peptide [GS17C (*14*)], we have recently shown that sufficient free CaM is indeed available in smooth muscle cells for interacting with CaD, thus supporting a physiological role for the CaM−CaD complex (*15*). A mechanism for CaM-based inhibition of CaD binding to actin is suggested by the closeness of the CaM-binding sites and the actin-binding sites in the amino acid sequence of CaD (*7*). A putative regulatory mechanism is likely to involve some conformational changes in addition to simple steric blocking, although the nature of such a conformational effect is not clear.

Another possible way to regulate CaD's action is through phosphorylation (*16*). One class of enzymes known to act on CaD consists of mitogen-activated protein kinases (MAPKs) (*17*), which add a phosphate group to serine residues at

† This work was supported by a grant from the National Institutes of Health (P01-AR41637).

* To whom correspondence should be addressed. Telephone: (617) 658-7803. Fax: (617) 972-1753. E-mail: wang@bbri.org.

‡ These authors contributed equally to this work.

[1] Abbreviations: CaD, caldesmon; CaM, calmodulin; DAB-Mal, 4-(dimethylamino)phenylazophenyl-4′-maleimide; DTT, dithiothreitol; ERK, extracellular signal-regulated kinase; FRET, fluorescence resonance energy transfer; IAEDANS, 5-(iodoacetamidoethyl)aminonaphthalene-1-sulfonic acid; MALDI-TOF, matrix-assisted laser desorption ionization time-of-flight; MAPK, mitogen-activated protein kinase; MS, mass spectrometry; PMSF, phenylmethanesulfonyl fluoride.

10.1021/bi0268605 CCC: $25.00
Published on Web 02/13/2003

positions 759 and 789 near the C-terminus of mammalian CaD (*18*). Although MAPK phosphorylation of CaD indeed occurs in vivo when smooth muscle is stimulated (*19*−*21*), its physiological significance is still controversial (*22*−*24*). Conflicting results have been reported on whether CaD's ability to inhibit the actomyosin ATPase activity is affected by phosphorylation (*25*−*27*). Evidence has also been lacking, apart from one recent report (*27*), that phosphorylation of CaD would result in any significant change in the affinity for F-actin (*28*).

In this work, we have examined the effects of Ca^{2+}/CaM and MAPK phosphorylation on CaD binding to actin, using fluorescence (or Förter) resonance energy transfer (FRET) and mass spectrometry coupled with proteolysis and cosedimentation experiments. We found that the C-terminal CaD fragment interacts with actin via multiple actin contact points that may be grouped into two clusters. Binding of CaM stabilizes an extended structure of the C-terminal region and maintains the separation of these two clusters, rendering CaD unable to interact with actin. Phosphorylation, on the other hand, results in dissociation of only one of the two actin-binding clusters, leaving the other cluster bound to actin. Both mechanisms necessitate a conformational change that may play a role in modulating the CaD's inhibitory effect.

MATERIALS AND METHODS

Cloning and Expression of C-Terminal Fragments of CaD. The C-terminal region of chicken CaD [H32K, residues M563−P771, using the corrected numbering system (*29*)] was subcloned into a pET28 vector with a His_6 tag at the N-terminus. A variant of the C-terminal fragment (H32Kqc) was also prepared with Q766 mutated to Cys. Both H32K and H32Kqc were expressed in BL21 *Escherichia coli* cells and purified with DE52 and CaM-Sepharose columns. A similar C-terminal fragment (h-H32K) corresponding to residues L604−V793 of human CaD was subcloned into a Bac-to-Bac vector (pFASTBacHTb, from Gibco) with a His_6 tag at its N-terminus, and expressed in High-Five cells. The overexpressed protein was purified from the insect cells on a Ni^{2+} column followed by a CaM affinity column. The purified CaD fragment expressed in insect cells tended to form aggregates more easily than the bacterially expressed fragment, but no other differences in binding properties were detected.

Labeling of H32Kqc. Purified and freshly reduced H32Kqc (19 μM) was first labeled with IAEDANS (10 μM). Part of the AEDANS-labeled sample was used as the control. The remaining sample continued to react with DAB-Mal (120 μM), followed by dialysis. In the final sample, [H32Kqc] = 6 μM, $[AEDANS]_{incorp} \sim 3.0$ μM, and $[DAB]_{incorp} = 8.5$ μM. To determine the position of the label, unlabeled H32Kqc and that stoichiometrically labeled with AEDANS were examined by mass spectrometry following digestion with V8 protease (see below). The species with a mass of 2054 Da (K590−E607, which contains C595) present in the digest of the unlabeled protein disappeared, with the concomitant emergence of a new peak at 2360 Da, consistent with it being the labeled segment (2054 Da plus the mass of the AEDANS moiety, 306 Da). A short piece of *m*/*z* 1294 (corresponding to the C766-containing segment of residues T761−P771) was found, as in the digest of the unlabeled H32Kqc, whereas the labeled species (*m*/*z* 1600) was not detected. Thus, it appeared that the donor group (AEDANS) was primarily attached to C595, even though no effort was made to achieve site-specific labeling, presumably because of the differential reactivity of the two thiols. Both AEDANS-labeled and unlabeled H32Kqc were also examined (in terms of their ability to bind CaM) by fluorescence titration (excitation wavelengths of 295 and 336 nm for Trp and dansyl emission, respectively). Trp fluorescence exhibited a blue shift upon addition of Ca^{2+}/CaM and was fully reversible with EDTA. The level of dansyl emission increased 60%, which was also reversible (data not shown).

Fluorescence Resonance Energy Transfer. Distance measurements by FRET followed established procedures (*30*−*32*). The transfer efficiency, *E*, was obtained by measuring the effect of the acceptor (DAB) on the fluorescence lifetime of the donor (AEDANS), and applying the equation

$$E = 1 - \tau_{da}/\tau_{d}$$

where τ_d and τ_{da} are donor fluorescence lifetimes in the absence and presence of the acceptor, respectively. The donor−acceptor separation distance (*r*) was obtained from the Förster equation (*33*, *34*):

$$r = R_o(E^{-1} - 1)^{1/6}$$

where R_o, the critical transfer distance, at which $E = 0.5$, is given by

$$R_o = [(8.79 \times 10^{-5})\kappa^2 n^{-4} Q J]^{1/6}\ \text{Å}$$

J, the overlap integral between the donor emission and acceptor absorption spectra, and Q, the donor quantum yield, were measured independently by spectroscopic methods; *n*, the refractive of the medium, was taken to be 1.36, a typical value for protein solutions, and κ^2, the orientation factor, was taken to be $^2/_3$, the isotropically averaged value. As described previously (*35*), the AEDANS−DAB-Mal donor−acceptor pair has a critical transfer distance of ~40 Å.

Mass Spectrometric Analysis. Digestion of H32Kqc or h-H32K was carried out at room temperature for 5−15 min in a buffer containing 20 mM Tris-HCl (pH 7.5), 50 mM KCl, 1 mM $CaCl_2$, 1 mM DTT, and 5 μM leupeptin, using V8 protease (1:20, w/w; from Sigma) in 0.1 mM PMSF or α-chymotrypsin (1:500, w/w; from Sigma) in 0.1 mM diisopropyl fluorophosphate. Diisopropyl fluorophosphate (for V8) or PMSF (for chymotrypsin) was added to stop the reaction. After digestion, the peptide solution was mixed with a saturated matrix solution (α-cyano-4-hydroxycinnamic acid in an acetonitrile/trifluoroacetic acid mixture) and spotted onto a 100-well stainless steel plate. Mass spectrometric analysis was then performed on a MALDI-TOF mass spectrometer (PerSeptive Biosystems Model Voyager-Elite with Delayed Extraction Technology) primarily in linear mode. The accelerating voltage was typically set at 20 kV. A nitrogen laser with intensity at 1500−2500 was used. Other settings were as follows: grid voltage of 93.5%, guide wire voltage of 0.200%, delay time of 150 ns, and source chamber pressure of $\sim 2 \times 10^{-7}$ Torr. Spectra were obtained by averaging 160−230 scans. The instrument was calibrated externally with insulin as a molecular mass standard.

ERK2 Phosphorylation. The 42 kDa extracellular signal-regulated kinase (ERK2), a member of the MAPK family, was used to elicit CaD phosphorylation. Typically, a 20 μL sample of h-H32K [14 μM in 20 mM Tris-HCl (pH 7.5), 50 mM KCl, 1 mM $CaCl_2$, 1 mM DTT, 5 μM leupeptin, and 0.1 mM PMSF] was treated at room temperature with 4 μL of recombinant ERK2 [from BioLabs, Inc., catalog no. P6080S, 2000 units in 20 μL of buffer containing 100 mM NaCl, 50 mM Tris-HCl (pH 7.5), 0.1 mM EDTA, 1 mM DTT, and 50% glycerol]. To the mixture were added 2.7 μL (to make a total volume of 27 μL) of a stock (10×) solution of reaction buffer [1× buffer contains 50 mM Tris-HCl (pH 7.5), 10 mM $MgCl_2$, 1 mM EGTA, and 2 mM DTT] and 0.15 mM ATP. For the sample used in the ATPase activity measurements (see below), 100 μL of the h-H32K stock and 10 μL of the ERK2 solution were used. In this case, the reaction took a longer time to complete because of a lower enzyme:substrate ratio. To monitor the extent of phosphorylation, aliquots (2 μL) of the reaction mixture were taken out at various time points and treated with V8 protease (1:20, w/w) at room temperature for 10 min, followed by MALDI mass spectrometric analysis. The phosphorylated CaD fragment appeared to be stable. There was no evidence of dephosphorylation throughout the course of all experiments, including cosedimentation with F-actin and ATPase activity assays.

Actin Binding Assays. Purified H32K or h-H32K (3−4 μM) was partially digested with V8 protease (for 5 min at room temperature), and subjected to cosedimentation with 57 μM rabbit skeletal muscle F-actin (with or without 8 μM chicken gizzard tropomyosin), in a solution containing 2 mM HEPES (pH 7.5), 50 mM NaCl, 2 mM $MgCl_2$, 0.2 mM $CaCl_2$, 0.5 mM DTT, and 0.4 mM ATP (F-buffer). Centrifugation was performed in a TL-100 rotor at 100000*g* for 30 min at 4 °C. Both the supernatant and the pellet fractions, the latter being washed three times with the same buffer, along with the total digest before mixing with F-actin, were analyzed by MALDI mass spectrometry. For testing the effect of CaM, the digest mixture of H32K was added with CaM (30−40 μM) in the presence of 0.2 mM $CaCl_2$ or 1 mM EGTA before ultracentrifugation. For competition experiments, samples containing equimolar (5 μM) H32K and actin in F-buffer were mixed with varying amounts of untreated or F-actin-treated (to remove the actin-binding peptides) total V8 or the chymotryptic digest (15 min at room temperature; see above) of H32K, ultracentrifuged after incubation, and analyzed by SDS−PAGE. The reciprocal control experiment was carried out by addition of the uncleaved H32K fragment to the digest prior to actin cosedimentation, followed by mass spectrometric analysis.

Actomyosin ATPase Activity Assay. Rabbit skeletal actin (3 or 7 μM) and gizzard tropomyosin (0.43 or 1 μM), in the presence or absence of equimolar (3 or 7 μM) unphosphorylated or ERK2-phosphorylated h-H32K, were incubated with rabbit skeletal muscle myosin (0.3 μM) or chicken gizzard smooth muscle myosin (0.7 μM). In the case of smooth muscle myosin, the light chains were phosphorylated by recombinant smooth muscle myosin light chain kinase expressed in insect cells (a gift from Z. Grabarek). The reactions were initiated by addition of 2 mM ATP. Release of inorganic phosphate (10 min at 37 °C) was assessed in quadruplicate by using an improved molybdate method (*36*) on microtiter plates. Reaction mixtures without actin or myosin were used as controls. Additional controls were performed using unphosphorylated smooth muscle myosin.

RESULTS

Identification of Actin-Binding Sites. MALDI mass spectrometry coupled with proteolysis and actin cosedimentation was used to identify the actin-binding sites of CaD. H32Kqc was treated with either V8 protease or α-chymotrypsin. The digests were then mixed with F-actin and centrifuged. Both the supernatant and pellet fractions were subjected to mass spectrometric analysis. On the basis of the known amino acid sequence and the cleavage specificity (at glutamic acid residues for V8 and at aromatic and leucine residues for chymotrypsin), the digestion products were predicted along with calculated masses using a computer program [Protein-Prospector, version 3.4.1; http://prospector.ucsf.edu (*37*)] allowing for multiple missed cuts. The peptide species displayed on the mass spectra were thus identified by comparing their observed masses with the predicted ones.

For both proteases, the mass spectra of the supernatants contained considerably more species than the pellet fractions. Since actin binding was not expected to be complete because of moderate affinities (*9*), only the peptides present in the pellet fractions were analyzed. There were five CaD peptides in the V8 digest, with masses of 2054, 2707, 3045, 3563, and 3883 Da, corresponding to the peptide residues K590−E607, G714−E738, F611−E638, W707−E738, and Q639−E675, respectively. These peptides were therefore taken to be the actin-binding segments. In the pellet of the chymotryptic digest, four CaD peptides were recognized, 2057, 3190, 3654, and 4138 Da, corresponding to the actin-binding segments of residues K594−F611, L612−Y640, E738−P771, and T641−F680, respectively (Figure 1 and Table 1). Inclusion of tropomyosin did not appreciably change the results. The N-terminal peptides containing the His_6 tag and the linker sequence were not found in the pellets, indicating that the engineered tag does not bind actin. In the control experiments, pellet fractions resulting from mixtures with either the CaD fragment or F-actin deleted did not have any peaks in the mass range of interest.

To test whether the interaction between the cleaved CaD fragments and actin is specific, we have performed competition experiments. For both V8 protease and chymotryptic cleavages, the digestion mixtures were able to quantitatively displace the undigested H32K from actin filaments (Figure 2). However, if the actin-binding peptides in the digests were removed by prior cosedimentation with F-actin, then the remaining substances in the supernatants were no longer effective in competing with the CaD fragment (lanes 7 and 8 in Figure 2). Conversely, uncleaved H32K was also able to displace all the actin-binding peptides in the digests from actin filaments without preference (data not shown). Thus, the observed actin binding activity for the individual peptides resulting from proteolytic digestions indeed reflects the properties of the intact CaD fragment, and not an artifact.

Notably, the peptides resulting from two independent enzymatic cleavages yielded similar actin-binding regions in the H32K sequence (Figure 1). These results, therefore, strongly suggested that each of these segments indeed contains actin-binding elements, thus supporting the idea that

FIGURE 1: Actin-binding clusters in H32Kqc (top sequence) and h-H32K (bottom sequence) determined by mass spectrometry in combination with proteolysis and actin cosedimentation. The actin-binding peptides generated by cleavages with V8 protease (under the sequence) or chymotrypsin (above the sequence), identified in the pellet fractions, are marked with thin black lines. The combined stretches of amino acid sequences covering all these actin-binding peptides are marked with thick gray lines. Note that in both isoforms there is a gap between the two clusters of actin-binding sites. The avian (top) and mammalian sequences (bottom) are ~80% identical in this region, although there are both conserved (highlighted in gray) and nonconserved (highlighted in yellow) amino acid replacements. The peptide segments in light gray are added His_6 tags and linkers that do not belong to the CaD sequence. Also included in this diagram are the cysteine residues (in bold black), ERK-phosphorylatable serines (in bold red), and the previously reported GS17C peptide, the CaM-binding sites (green boxes) and actin-binding site (black box).

Table 1: Pepides Identified in the Pellet Fractions by Mass Spectrometric Analysis after Cosedimentation of Proteolyzed CaD Fragments with F-Actin

CaD sample	protease	M_r (calcd)	M_r (obs)[a]	amino acids[b]
H32Kqc	V8	2054.5	2055.0	590−607
		2707.0	2707.8	714−738
		3045.5	3046.1	611−638
		3563.0	3564.0	707−738
		3883.5	3884.2	639−675
	α-chymotrypsin	2057.4	2058.0	594−611
		3189.7	3190.4	612−640
		3654.1	3655.3	738−771
		4137.8	4138.6	641−680
h-H32K	V8	3516.0	3515.8	649−680
		3579.0	3579.9	749−780
		3960.5	3959.2	681−717
		4854.5	4854.1	688−734
		4977.7	4976.3	749−793

[a] The observed masses are all within 0.03% of the calculated ones. [b] For H32Kqc, the corrected chicken gizzard sequence numbering system was used; for h-H32K, the human smooth muscle CaD sequence was used.

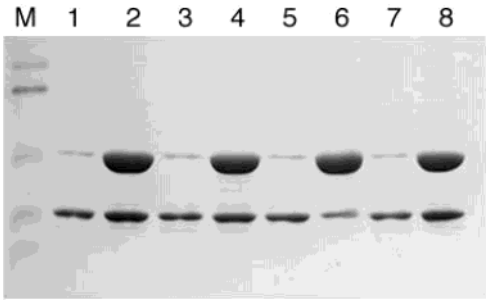

FIGURE 2: Competition between digested and undigested H32K for actin binding. Samples containing equimolar (5 μM) H32K and actin in F-buffer (see Materials and Methods; total volume of 200 μL each) were incubated either alone (lanes 1 and 2) or with 5 (lanes 3 and 4) or 10 μM (lanes 5 and 6) of total V8 digest of H32K (lanes 3−6) or the supernatant of the same digest (10 μM) that had been previously cosedimented with F-actin (lanes 7 and 8). After ultracentrifugation, both the supernatant (40 μL out of 200 μL, lanes 1, 3, 5, and 7) and pellet (the entire material dissolved in 20 μL of buffer, lanes 2, 4, 6, and 8) fractions were analyzed by PAGE in the presence of SDS. Lane M contained molecular mass markers.

multiple actin contact points exist in the C-terminal region of CaD. Furthermore, these discrete actin-binding segments fall into two clusters of actin-binding sites (from K590 to F680 and from W707 to P771), separated by a "gap". The peptides (*m*/*z* 1431, or T693−E706, for the V8 digest and *m*/*z* 2731, or S681−W707, for the chymotryptic digest) that comprise the gap were indeed found in the supernatant but not in the pellet fractions, confirming that this segment lacks actin binding properties. We have performed the same experiments with the mammalian analogue h-H32K. Similar results were obtained (Table 1). There was also a gap (from T735 to E748) that corresponds to the same sequence as that in the chicken isoform, separating two actin-binding clusters [residues D630−E734 and W749−V793 (Figure 1)].

Effect of Ca^{2+}/CaM. To test the effect of CaM on the actin binding properties of the cleaved CaD fragment, we have added Ca^{2+}/CaM to the V8 digest of H32Kqc prior to cosedimentation with F-actin, and examined the pellets by mass spectrometry. It should be pointed out that mass spectrometry has been generally regarded as a tool for only qualitative analyses. However, as shown previously (*38*, *39*), quantitative MALDI-MS is possible if there is an internal standard, and if the peak ratios between the analytes and the standard are compared. In the present case, peaks not affected by CaM were used as internal standards.

We found that only the peak with a mass of 2054 Da in the pellet fraction exhibited a 50% decrease in the intensity relative to the other four peaks. This suggests that binding of the peptide segment of K590−E607 to F-actin is somewhat weakened by Ca^{2+}/CaM, whereas all the other peptides are not affected. The CaM-induced decrease in the level of actin binding of the 2054 Da peptide was fully reversed by EGTA. Although there has been no evidence that this segment (K590−E607) itself binds CaM, it does contain an endogenous Cys residue (C595), which, when labeled with a photo-cross-linker (benzophenyl maleimide), was shown to cross-link to CaM (*40*). It is rather surprising that most of the actin-binding peptides are not affected, considering that under the same conditions, undigested H32K

Table 2: Lifetime Measurements of Singly and Doubly Labeled H32Kqc

sample	lifetime (ns)[a]	*r* (Å)
$H32K_{AEDANS}$	14.03	
$H32K_{AEDANS}$ with Ca	13.99	
$H32K_{AEDANS}$ with Ca and CaM	14.28	
$H32K_{AEDANS}$ with Ca, CaM, and EDTA	14.14	
$H32K_{AEDANS}$ with actin	15.37	
$H32K_{AEDANS}$ with actin and Ca	15.41	
$H32K_{AEDANS}$ with Ca, actin, and CaM	14.84	
$H32K_{AEDANS}$ with Ca, actin, CaM, and EGTA	15.17	
$H32K_{AEDANS/DAB}$	13.15	62.8
$H32K_{AEDANS/DAB}$ with Ca	12.89	60.4
$H32K_{AEDANS/DAB}$ with Ca and CaM	13.47	64.0
$H32K_{AEDANS/DAB}$ with Ca, CaM, and EDTA	13.03	60.4
$H32K_{AEDANS/DAB}$ with actin	10.92	46.4
$H32K_{AEDANS/DAB}$ with actin and Ca	10.93	46.4
$H32K_{AEDANS/DAB}$ with Ca, actin, and CaM	13.83	62.0
$H32K_{AEDANS/DAB}$ with Ca, actin, CaM, and EGTA	11.26	47.6
phospho-$H32K_{AEDANS}$	14.47	
phospho-$H32K_{AEDANS}$ with actin	15.00	
phospho-$H32K_{AEDANS/DAB}$	13.92	68.5
phospho-$H32K_{AEDANS/DAB}$ with actin	13.70	59.2

[a] The decay data points (Figure 3) were fitted by two-exponential methods-of-moments analysis to obtain both lifetimes and amplitudes. Only the best-fit lifetimes of the major component are reported here. The estimated error in lifetime measurements was ∼5%.

would have been completely displaced from the actin filament by CaM in the presence of Ca^{2+}. Apparently, when cleaved into separate peptides, these actin-binding segments behave quite independently. Breaks in the linkages among these segments may also disable some conformational changes that are needed for CaM-induced CaD dissociation from actin (see below).

CaM- and Actin-Induced Conformational Changes by FRET. To investigate the effect of actin or CaM binding on the conformation of the CaD fragment, we have carried out intramolecular distance measurements by FRET. H32Kqc was labeled at the two cysteine residues (C595 and C766) with IAEDANS as the donor, and DAB-Mal as the acceptor. The emission of AEDANS attached to H32Kqc (at C595; see Materials and Methods) decayed in the absence of the acceptor with a single lifetime of 14.0 ns. This lifetime was not affected (14.1 ± 0.1 ns) by the addition of Ca^{2+} or CaM, but became somewhat longer (15.2 ± 0.3 ns) when actin was present (see Table 2). The change in lifetime could reflect a different environment of the probe, because of either added protein or a conformational change. When the protein was also labeled with DAB-Mal at the remaining available thiol (C766), the AEDANS lifetime was only slightly shortened to 13.2 ns. From this lifetime and that of $H32K_{AEDANS}$ under the same condition, the distance separation (*r*) was calculated between the two probes, assuming that the lifetime change resulted from FRET between the donor (AEDANS) and the acceptor (DAB) moieties. We have obtained an interprobe distance of 62.8 Å between C595 and C766 for an isolated C-terminal CaD fragment. The same procedure was repeated for other experimental conditions.

We found that the donor−acceptor distance in doubly labeled H32Kqc ($H32K_{AEDANS/DAB}$) was not affected by the addition of Ca^{2+}, and was slightly increased (from 62 to 64 Å) when CaM was added. However, when F-actin was added to $H32K_{AEDANS/DAB}$, the AEDANS emission decayed with a much shorter lifetime of 10.9 ns (Figure 3). This indicated that the efficiency of FRET is increased due to a conformational change that brings the two probes closer, to ∼46.4 Å. Addition of Ca^{2+}/CaM apparently abolished this structural change, and caused the interprobe distance to return to 62 Å. Further addition of EGTA reinstated the actin-induced conformational change (Figure 3 and Table 2). The reciprocal effect of Ca^{2+}/CaM and EGTA is consistent with the previous observation that CaM caused dissociation of CaD from actin in a Ca^{2+}-dependent manner. The new finding here is that such dissociation is mediated by an extension of the C-terminal region of CaD.

Detection of Phosphorylation by Mass Spectrometry. Although phosphorylation, which results in a mass increase of 80 Da (H_2PO_4 replacing OH), is difficult to discern on a protein by mass spectrometry, it is readily detectable when the molecule is cleaved into smaller fragments (*41*). To test the effect of phosphorylation on the actin binding properties of CaD, we have used a homologous fragment, h-H32K, corresponding to the C-terminal region of human smooth muscle CaD. There are two ERK phosphorylation sites in h-H32K: S759 and S789. In the mass spectrum of the peptides resulting from V8 digestion of unphosphorylated h-H32K, we found peaks with apparent masses of *m*/*z* 3579 (M) and 4977 (M′); the former represents residues 749−780, which includes a single phosphorylation site (S759), whereas the latter corresponds to residues 749−793, which includes both S759 and S789.

When h-H32K was treated with ERK2 prior to V8 proteolysis, three additional peaks were detected at *m*/*z* 3659 (M + 80), 5057 (M′ + 80), and 5137 (M′ + 160), corresponding to the singly and doubly phosphorylated species of the Ser-containing fragments. The appearance of these phosphorylated peaks (denoted with asterisks in Figure 4, top panel) was accompanied by a concomitant decrease in the intensity of the parent peaks. The relative peak intensity of these new species increased as a function of time and followed a saturation curve (Figure 5), consistent with the anticipated kinetics of the phosphorylation reaction. Quantification of the extent of phosphorylation was achieved by using, as internal standards, peptides that were not affected by phosphorylation, such as the peaks at *m*/*z* 3516 and 4854, corresponding to the fragments of residues 649−680 and 688−734 (Table 3), respectively.

Effect of ERK Phosphorylation on the Actin Binding Properties of CaD. When the digestion mixtures of both unphosphorylated and ERK2-phosphorylated h-H32K were cosedimented with F-actin, and the pellet and supernatant fractions of each digest were examined by mass spectrometry, both the peaks with masses of 3579 Da (Figure 6A) and 4977 Da (Figure 6C) were found in the pellet, whereas the peaks with masses of 3659 Da (Figure 6B) and 5057 and 5137 Da (Figure 6D) were present mainly in the supernatant, and virtually absent in the pellet. These results indicate that peptides of both residues 749−780 and 749−793 are able to interact with F-actin, but the interaction is severely weakened when S759 and/or S789 becomes phosphorylated.

We noticed that in the spectrum of the h-H32K digest before ERK2 treatment, there was also a small peak at *m*/*z* 5057 (Figure 6C, asterisk), suggesting that one of the two serine residues is phosphorylated in the insect cells. This peak was also found only in the supernatant fraction but not

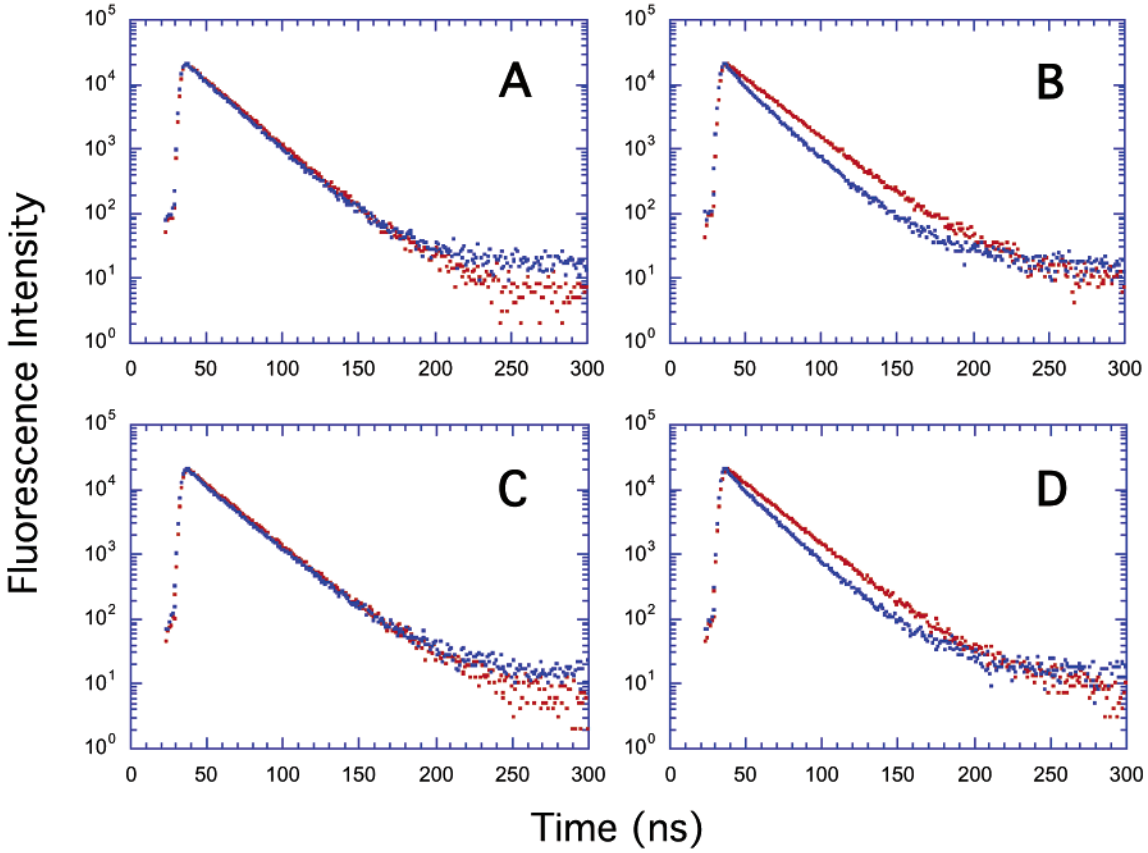

FIGURE 3: Fluorescence decay data of $H32K_{AEDANS}$ in the presence (blue) and absence (red) of the acceptor DAB under various conditions. (A) Singly and doubly labeled H32Kqc alone, (B) H32Kqc with F-actin, (C) H32Kqc with F-actin and CaM in 0.5 mM $CaCl_2$, and (D) H32Kqc with F-actin and CaM in 1 mM EGTA. The dots are experimental data points, which were fitted by methods-of-moments analysis to obtain lifetimes (Table 2).

in the actin pellet (Figure 6C), like that obtained after ERK2 treatment (Figure 6D). Since the peak at *m*/*z* 3659 was not detected in the same spectrum (Figure 4A), S759 was not modified, and therefore, S789 must be the one that is phosphorylated in the insect cell. We have confirmed this conclusion by Western blot analysis. Untreated h-H32K did react with an antibody raised against a phosphopeptide containing S789, but did not react with an antibody against a phosphopeptide containing S759 (ref *42* and data not shown). Interestingly, this site (S789) was also found to be constitutively phosphorylated in porcine carotid arteries (*42*). Moreover, the 5057 Da peptide (corresponding to residues 749−793) contains the segment of residues 749−780 (*m*/*z* 3581) which by itself binds actin (Figure 6A). The fact that the 749−793 peptide fails to bind F-actin upon phosphorylation at S789 alone suggests that addition of a phosphate group at S789 outside the 749−780 peptide is sufficient to abolish its binding to actin. Such a long-range effect is significant, because it represents a conformational change, not merely a charge effect. It also suggests that phosphorylation at S789 may play a significant role in ERK-induced regulation.

Although ERK phosphorylation has been suggested to be a plausible mechanism for the reversal of CaD-induced inhibition, there have been no clear data, even in vitro, to indicate that such phosphorylation would significantly change the affinity of CaD for F-actin (*28*). Our data appear to provide an explanation for this apparent paradox. As shown above, the multidomain CaD molecule contains multiple actin contact points in the C-terminal region. Clearly, not all actin contact points are simultaneously affected by ERK phosphorylation; those sites remaining bound to F-actin after ERK treatment, such as residues 649−680 (*m*/*z* 3516) and 688−734 (*m*/*z* 4854), could render the detection of any change in overall binding by cosedimentation assays difficult (Figure 6). This conclusion is in agreement with a recent study using NMR spectroscopy (*27*).

Effect of Phosphorylation on the Conformation of CaD. Since ERK phosphorylation can partially dissociate CaD from F-actin, one would like to know whether such an effect results from a conformational change in the C-terminal region of CaD similar to that induced by Ca^{2+}/CaM. We have addressed this issue with FRET experiments on both the phosphorylated and unphosphorylated CaD fragments. H32Kqc doubly labeled with the donor (IAEDANS) and acceptor (DAB-Mal) was first phosphorylated with ERK2 and subjected to lifetime measurements. The level of phosphorylation was ascertained to be nearly 100% complete by mass spectrometric analysis. As shown in Table 2, incorporation of a phosphate group at S717 was accompanied by a moderate (6 ± 2 Å) elongation in H32Kqc. Upon addition of F-actin, the separation between C595 and C766 decreased from 68.5 to 59.2 Å. Although this represents a significant contraction in the overall molecule, the resultant conformation is still more extended than the actin-bound, unphosphorylated protein (46.4 Å). Thus, ERK2-induced phosphorylation and CaM binding have similar, although not identical, effects on the structure of CaD. The ~10 Å

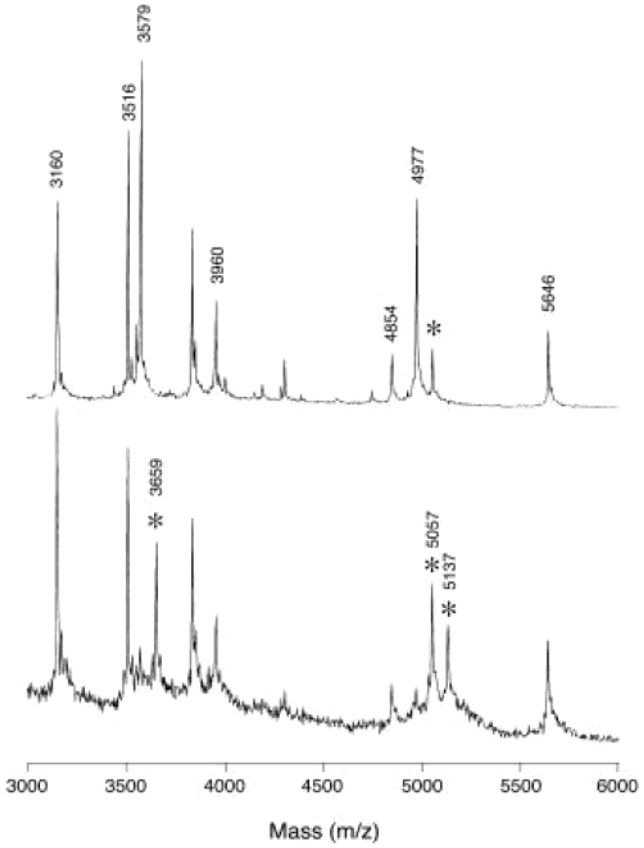

FIGURE 4: Mass spectra of V8-digested h-H32K before (top panel) and after (bottom panel) ERK2 treatment. All major CaD peptides in the mass range of *m*/*z* 3000−6000 Da are identified. Note that peaks at *m*/*z* 3579 and 4977 correspond to peptide segments containing serine residues that can be phosphorylated by ERK2 (see Table 1 and the text). Peaks denoted with asterisks are the phosphorylated species of these two peptides.

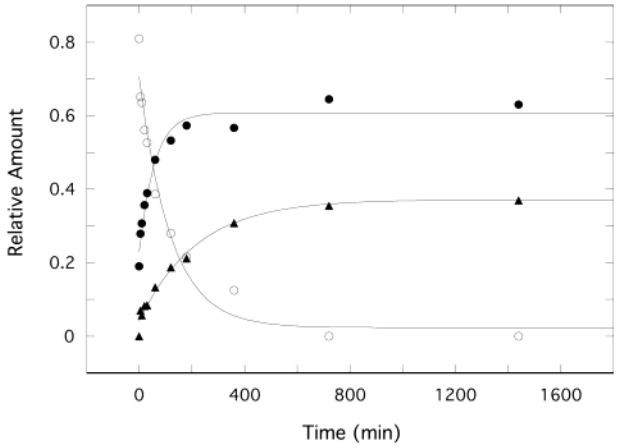

FIGURE 5: Time course of phosphorylation of h-H32K by ERK2. h-H32K was treated with ERK2 in the presence of ATP. At various time points, an aliquot of the reaction mixture was taken and digested with V8 protease at room temperature for 10 min, followed by MALDI mass spectrometric analysis (see Materials and Methods). The peak intensities of unphosphorylated (*m*/*z* 3579 and 4977), singly phosphorylated (*m*/*z* 3659 and 5057), and doubly phosphorylated (*m*/*z* 5137) species were measured, and normalized against the intensity of the peak at *m*/*z* 3516 in each respective mass spectrum. The fractions of all three groups [unphosphorylated (○), singly phosphorylated (●), and doubly phosphorylated (▲)], relative to the total amount of both phosphorylated and unphosphorylated species, were plotted as a function of time. Smooth curves were drawn through the data points only to show the trend. It should be pointed out that, since the 749−780 segment (*m*/*z* 3579 or 3659) is derived from the longer 749−793 segment (*m*/*z* 4977, 5057, or 5137), the 3659 Da species could be from either singly phosphorylated (at S759) or doubly phosphorylated h-H32K; for the same reason, the apparently "unphosphorylated" species at *m*/*z* 3579 could be from singly phosphorylated (at S789) h-H32K. The relative abundance of these two segments in a given sample depends on the extent of V8 digestion, which was kept the same in this experiment.

shortening in the interprobe distance upon actin binding for the phosphorylated protein may correspond to a conformational change in the region of the actin-binding cluster that contains no phosphorylation sites (see the Discussion below).

Effect of Phosphorylation on the Inhibitory Properties of CaD. Although a number of actin contact points were not affected by ERK phosphorylation, the loss of actin binding for those peptides containing phosphorylatable serine (e.g., residues 749−780 and 749−793) appeared to be sufficient for removal of inhibition. It has previously been reported that the inhibitory region resides in the extreme C-terminal segment of gizzard CaD (*7*); thus, ERK phosphorylation may be able to result in a regulatory effect. We therefore tested whether ERK phosphorylation affects the ability of CaD to inhibit the actomyosin ATPase activity. As shown in Table 4, at a molar ratio of h-H32K to actin of 1:1, unphosphorylated h-H32K inhibits 63−67% of the actin-activated ATPase activity of either rabbit skeletal muscle myosin or phosphorylated chicken gizzard smooth muscle myosin. However, the level of inhibition progressively decreased with time as h-H32K was being treated with ERK2. In the case of smooth muscle myosin, overnight incubation of the CaD

Table 3: Identification of the CaD Peptides Resulting from V8 Digestion[a]

peptide sequence	M_r[b]	amino acids[c]
TAGLKVGVSSRINE	1431.6	735−748
KGNVFSSPTAAGTPNKE	1705.9	718−734
FLNKSVQKSSGVKSTHQAAIVSKIDSRLE	3159.6	652−680
RAEFLNKSVQKSSGVKSTHQAAIVSKIDSRLE	3516.0	649−680
WLTKTPDGNK**S**PAPKPSDLRPGDVSSKRNLWE	3579.0	749−780[d]
AAEKRQKMPEDGLSDDKKPFKCFTPKGSSLKIEE	3840.4	615−648
QYTSAIEGTKSAKPTKPAASDLPVPAEGVRNIKSMWE	3960.5	681−717
GTKSAKPTKPAASDLPVPAEGVRNIKSMWEKGNVFSSPTAAGTPNKE	4854.5	688−734
WLTKTPDGNK**S**PAPKPSDLRPGDVSSKRNLWEKQSVDKVT**S**PTKV	4977.7	749−793[d]
QYTSAIEGTKSAKPTKPAASDLPVPAEGVRNIKSMWEKGNVFSSPTAAGTPNKE	5647.4	681−734

[a] The observed mass numbers of peaks in the mass spectrum were compared with the calculated ones on the basis of the cleavage specificity of V8 protease. For unphosphorylated CaD, at least 10 species in the mass range of 1400−6000 Da were identified. [b] The observed masses are all within 0.03% of the calculated ones. [c] Human smooth muscle CaD sequence. [d] Fragments containing phosphorylatable serine residues (S759 and S789, shown in bold).

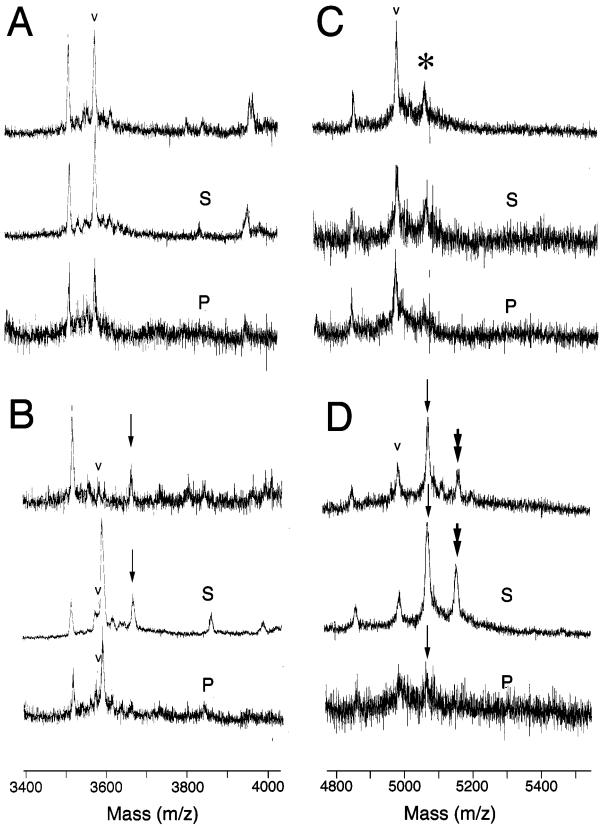

FIGURE 6: Effect of ERK2 phosphorylation on actin binding of h-H32K. h-H32K was first phosphorylated with ERK2, partially digested with V8 protease (for 5 min at room temperature), and subjected to cosedimentation with F-actin. Both the supernatant (S) and the washed pellet (P) fractions, along with the total digest before mixing with F-actin (top trace in each panel), were analyzed by MALDI mass spectrometry. (A and B) Partial mass spectra of V8-digested h-H32K in the region of ~3580 Da and (C and D) partial mass spectra of V8-digested h-H32K in the region of ~4980 Da before (A and C) and after (B and D) ERK2 treatment. The unphosphorylated species (*m*/*z* 3579 and 4977) were denoted by v. The large peak next to the 3579 Da species (trace S and trace P in panel B) was from actin. The unphosphorylated species in both regions were present in the pellet, indicating their actin binding properties. Peaks denoted with a single arrow (at *m*/*z* 3659 and 5057) are singly phosphorylated species; the peak denoted with a double arrow (at *m*/*z* 5137) is the doubly phosphorylated species. Note that all phosphorylated species were only found in the supernatant, but not (or very little) in the pellet fractions, suggesting actin binding is severely weakened by ERK phosphorylation. The peak at *m*/*z* 5057 before ERK2 treatment (denoted with an asterisk, panel C) is a species singly phosphorylated at S789 in insect cells, and exhibited very weak binding to F-actin.

Table 4: Effect of Unphosphorylated and Phosphorylated h-H32K on the Actomyosin ATPase Activity

	phosphorylation			
	time (h)	level (%)[a]	smooth myosin	skeletal myosin
control			1.00[b]	1.00[b]
h-H32K			0.36 ± 0.05	0.32 ± 0.04
h-H32K-**P**	2	42	0.53 ± 0.03	0.48 ± 0.07
	4	68	0.65 ± 0.09	0.61 ± 0.01
	18	86	0.83 ± 0.04	0.76 ± 0.03

[a] Estimated on the basis of mass spectrometric analysis. [b] The absolute activity of skeletal myosin was ~10 times higher than that of smooth myosin.

fragment with the kinase recovered nearly 75% of the lost actomyosin ATPase activity (from 36 to 83%). Simultaneous measurements of the resulting phosphopeptides by mass spectrometry showed that the reappearance of the ATPase activity correlates well with the level of phosphorylation (Table 4). Thus, addition of phosphate groups at S759 and S789 clearly weakens the inhibitory effect of h-H32K, most likely as a consequence of the growing inability of certain parts of this CaD fragment to interact with actin.

DISCUSSION

The actin binding property enables CaD in smooth muscles to play a functional role. The major actin-binding sites are located in the C-terminal region of CaD, although a weaker and heat-labile actin-binding site may exist in the N-terminal region of the molecule (*13*), the exact location of which has not yet been determined. CaD also binds to the monomeric form of actin. When added to G-actin, CaD accelerates polymerization (*43*, *44*). This phenomenon leads to the assumption that CaD interacts simultaneously with more than one actin subunit, and thereby decreases the critical concentration of actin nucleation. The presence of multiple actin-binding sites is supported by the observation that CaD bundles actin filaments (*45*, *46*). The fact that actin bundling is triggered even by a C-terminal fragment of CaD (*47*) indicates that these actin-binding sites are concentrated in the C-terminal region of the molecule. In fact, at least two actin-binding segments have been identified in a 100-residue segment near the carboxyl end (*7*, *48*, *49*). It has been suggested that the organization of these binding segments on actin defines the tertiary folding of this part of CaD (*49*, *50*).

Although there is general agreement among different research groups concerning the idea of multiple actin-binding sites, there is no consensus about the specific segments and sequences involved. By using internal deletion mutagenesis, Chacko's laboratory (*51*) came to the conclusion that there is one strong actin-binding site (K733−E738 in the corrected numbering system of gizzard CaD) and there are two weak ones (E665−S681 and N705−G714). NMR studies of Marston and associates (*49*, *52*), on the other hand, concluded that the "dual-sited attachment" on actin involves peptide segments I704−L708 (site B) and L736−Q740 (site B′), with a four-residue "turn" of G728−S731 between them. A comparison of these segments revealed that Chacko's strong site overlaps Marston's site B and one of their weak sites overlaps site B′, but the other more upstream actin-binding site (E665−S681) reported by Chacko et al. was not mentioned in the NMR work because a shorter fragment was used therein. This other site is included in the study presented here (Q639−E675 in the V8 digest and T641−F680 in the chymotryptic digest) and was also reported in our earlier work (*7*). Taken together, the actin-binding domain in the C-terminal region of CaD can be best described by two noncontiguous clusters, separated by a peptide stretch (S681−R703 for avian CaD and T735−E748 for the mammalian isoform), each cluster being made up of several smaller actin-binding segments. The two clusters most likely interact with two different actin subunits, which may be in the same filament, but could also be from two adjacent actin filaments (hence, bundling occurs).

The conclusion that two actin-binding clusters exist is consistent with the FRET results. Focusing on the chicken isoform, we have found that H32K is an elongated molecule,

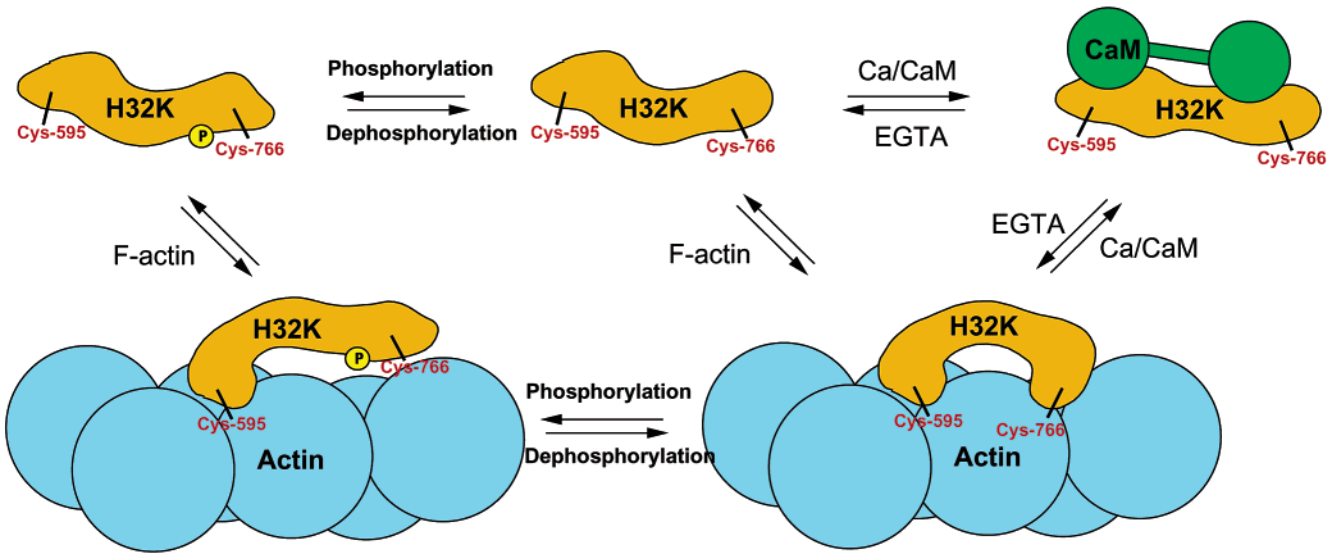

FIGURE 7: Schematic model depicting the two-pronged binding of the C-terminal region of CaD and the dual mode of conformational changes induced by CaM and ERK phosphorylation. Each of the two attachment points of H32Kqc on F-actin represents one of the two clusters of actin-binding sites. Binding of CaM leads to the dissociation of the entire CaD fragment from F-actin. ERK2 phosphorylation, on the other hand, induces a similar extension in H32Kqc, but only in the region that contains the phosphorylation site(s), thus resulting in the detachment of only one of the two clusters. Note that the actin subunits are drawn only for the purposes of illustration; the two clusters do not need to land on the same actin subunit.

in which probes attached to C595 and C766 are separated by a distance of 62 Å. Such an extended structure is apparently stabilized by CaM in the presence of Ca^{2+}. But once actin has bound, it undergoes a conformational change to assume a more compact structure in which the two Cys residues are brought ~15 Å closer. The fact that it takes two different conformers to interact with CaM and actin explains why binding of CaD to F-actin can be regulated by CaM in a Ca^{2+}-dependent manner. Also, as C595 and C766 are located in different actin-binding clusters, the conformational change may involve a movement that hinges on the connecting segment (Figure 7). Apparently, this connecting segment is essential for such a conformational change. Once the hinge is broken, as seen in the V8 digest (Figure 1), CaM can no longer completely displace all CaD peptides from actin. This mechanism is therefore different from the "flip-flop" model originally proposed by Sobue et al. (*53*).

According to previous studies (*7*, *51*), of the two actin-binding clusters the C-terminal one is involved in the inhibitory action of CaD. It is also this cluster in which the residues that can be modified by ERKs are located (*18*). Thus, if kinases such as ERKs are to play a regulatory role, one would expect the binding of this segment of CaD to actin to be affected by ERK phosphorylation. We have demonstrated in this report that this is indeed the case. Phosphorylation of the mammalian CaD fragment (h-H32K) by ERK2 at both Ser residues at positions 759 and 789 inhibits the actin binding ability of peptide segments containing these residues, whereas the affinity of peptide segments not containing these phosphorylatable serines is not affected. The latter finding, in particular, may explain the controversy in the literature that only a subtle difference in actin binding was observed when smooth muscle CaD was phosphorylated by MAPK (*28*). As shown by our data, ERK phosphorylation clearly reverses the ability of CaD to inhibit the actomyosin ATPase activity, in concert with a change in the mode of binding to actin. It might be advantageous kinetically for CaD to alleviate its inhibitory activity while remaining bound to F-actin so that upon dephosphorylation, it can quickly return to the inhibitory position. This may suggest a plausible mechanism by which ERK exerts a regulatory effect on the action of CaD. Such a mechanism may also find applications in other ERK-involved signaling pathways.

Mammalian CaD contains two phosphorylatable serine residues (S759 and S789) in the C-terminal region, whereas avian CaD contains only one (S717), which is in a position homologous to S759. Although our actin binding experiments were carried out with the human isoform, the conclusion should be applicable to chicken CaD as well, because the singly phosphorylated species (*m*/*z* 3659, corresponding to the peptide segment of residues 749−780, thus containing only S759) failed to cosediment with F-actin. This segment is identical to the chicken counterpart of residues 707−738 (containing S717) with only two residue replacements (D755 and G732 in mammalian CaD switched to E713 and S774 in the avian isoform, respectively; Figure 1).

The conformational change brought about by the phosphorylation could be similar to the one observed for CaM binding, i.e., a hinged movement of the segment between the two actin-binding clusters. However, because phosphorylation does not lead to total dissociation of the C-terminal fragment unless it is cleaved, such a conformational change may not necessarily be the same as the one induced by CaM. Indeed, we saw a further elongation of H32Kqc upon ERK phosphorylation (Table 2). When F-actin is present, the interprobe distance shrinks ~10 Å, but is still much greater than that in the unphosphorylated state (59 vs 46 Å). This is consistent with the idea that in the phosphorylated CaD only one of the two actin-binding clusters functions; the other one is disabled by the added phosphate group, most likely because of a charge-induced structural change (Figure 7). The disabled cluster does not change its structure and remains elongated in the presence of actin, whereas the active cluster

undergoes a conformational change that brings the two probes 10 Å closer. Our mass spectrometric analysis revealed that the cluster that remains active is the one more toward the upstream where no ERK-induced phosphorylation takes place. It is conceivable that if this region also became phosphorylated, CaD would completely dissociate from actin filaments. In fact, this was observed to be the case for non-muscle CaD when it is phosphorylated by $p34^{cdc2}$ kinase during mitosis at several Ser/Thr-Pro sites, including S724 and S730 in the first actin-binding cluster (*57*). Thus, this may provide a mechanism by which different functions of CaD are regulated by different kinases.

The partial dissociation of the C-terminal actin-binding cluster resulting from ERK phosphorylation alleviates its inhibition of the actomyosin ATPase activity (Table 4). The same observation was reported by Patchell et al. (*27*), although no data were presented. It is not clear why the previous studies failed to see such an effect. In fact, opposite results were observed (*26*, *54*), although ERK phosphorylation was indeed found to inhibit CaD's ability to inhibit the sliding velocity of actin filaments in the motility assay (*22*).

MAPK activation can occur in a Ca^{2+}-independent manner. The ERK-induced phosphorylation provides a mechanism for smooth muscle CaD to be regulated in the absence of a change in the calcium level. Together with CaM, whose action requires Ca^{2+}, MAPK may thus allow smooth muscle contractility to be fine-tuned under a variety of physiological conditions. Although direct evidence for the involvement of MAPK in smooth muscle regulation is still lacking, that possibility has not yet been ruled out (A. V. Vorotnikov, personal communication). Furthermore, it has been reported that MAPK phosphorylation of CaD in cultured cells is indeed relevant to cellular functions. Both smooth muscle and non-muscle CaD isoforms share an identical C-terminal region, as a result of alternative splicing from the same gene (*55*). As shown in recent studies (*42*, *56*), MAPK-dependent phosphorylation of CaD is involved in the growth and migration of cultured smooth muscle cells. Therefore, the information obtained in this study would also be useful in bringing us closer to a full understanding of the functions of CaD in non-muscle cells.

ACKNOWLEDGMENT

We thank Drs. Guanming Wu and Renne C. Lu for their help and advice on mass spectrometry and Drs. John Gergely, Zenon Grabarek, and Toshio Kitazawa for critical reading of the manuscript and valuable discussions.

REFERENCES

1. Clark, T., Ngai, P. K., Sutherland, C., Groschel-Stewart, U., and Walsh, M. P. (1986) Vascular smooth muscle caldesmon, *J. Biol. Chem. 261*, 8028−8035.
2. Szpacenko, A., Wagner, J., Dabrowska, R., and Ruegg, J. C. (1985) Caldesmon-induced inhibition of ATPase activity of actomyosin and contraction of skinned fibres of chicken gizzard smooth muscle, *FEBS Lett. 192*, 9−12.
3. Fujii, T., Imai, M., Rosenfeld, G. C., and Bryan, J. (1987) Domain mapping of chicken gizzard caldesmon, *J. Biol. Chem. 262*, 2757−2763.
4. Szpacenko, A., and Dabrowska, R. (1986) Functional domain of caldesmon, *FEBS Lett. 202*, 182−186.
5. Mezgueldi, M., Derancourt, J., Calas, B., Kassab, R., and Fattoum, A. (1994) Precise identification of the regulatory F-actin- and calmodulin-binding sequences in the 10-kDa carboxyl-terminal domain of caldesmon, *J. Biol. Chem. 269*, 12824−12832.
6. Bartegi, A., Fattoum, A., Derancourt, J., and Kassab, R. (1990) Characterization of the Carboxyl-terminal 10-kDa Cyanogen Bromide Fragment of Caldesmon as an Actin-Calmodulin-binding Region, *J. Biol. Chem. 265*, 15231−15238.
7. Wang, C.-L. A., Wang, L.-W. C., Xu, S. A., Lu, R. C., Saavedra-Alanis, V., and Bryan, J. (1991) Localization of the calmodulin- and the actin-binding sites of caldesmon, *J. Biol. Chem. 266*, 9166−9172.
8. Sobue, K., Morimoto, K., Inui, M., Kanda, K., and Kakiuchi, S. (1982) Control of actin-myosin interaction of gizzard smooth muscle by calmodulin and caldesmon-linked flip-flop mechanism, *Biomed. Res. 3*, 188−196.
9. Smith, C. W., Pritchard, K., and Marston, S. B. (1987) The mechanism of Ca^{2+} regulation of vascular smooth muscle thin filaments by caldesmon and calmodulin, *J. Biol. Chem. 262*, 116−122.
10. Walsh, M. P. (1987) Caldesmon, a major actin- and calmodulin-binding protein of smooth muscle, *Prog. Clin. Biol. Res. 245*, 119−141.
11. Shirinsky, V. P., Bushueva, T. L., and Frolova, S. I. (1988) Caldesmon-calmodulin interaction, *Biochem. J. 255*, 203−208.
12. Kasturi, R., Vasulka, C., and Johnson, J. D. (1993) Ca^{2+}, caldesmon, and myosin light chain kinase exchange with calmodulin, *J. Biol. Chem. 268*, 7958−7964.
13. Zhuang, S., Mabuchi, K., and Wang, C.-L. A. (1996) Heat treatment could affect the biochemical properties of caldesmon, *J. Biol. Chem. 271*, 30242−30248.
14. Zhan, Q., Wong, S. S., and Wang, C.-L. A. (1991) A calmodulin-binding peptide of caldesmon, *J. Biol. Chem. 266*, 21810−21814.
15. Hulvershorn, J., Gallant, C., Wang, C.-L. A., Dessy, C., and Morgan, K. G. (2001) Calmodulin levels are dynamically regulated in living vascular smooth muscle cells, *Am. J. Physiol. 280*, H1422−H1426.
16. Ngai, P. K., and Walsh, M. P. (1984) Inhibition of smooth muscle actin-activated myosin Mg^{2+}-ATPase activity by caldesmon, *J. Biol. Chem. 259*, 13656−13659.
17. Adam, L. P., Haeberle, J. R., and Hathaway, D. R. (1989) Phosphorylation of caldesmon in arterial smooth muscle, *J. Biol. Chem. 264*, 7698−7703.
18. Adam, L. P., and Hathaway, D. R. (1993) Identification of mitogen-activated protein kinase phosphorylation sequences in mammalian h-caldesmon, *FEBS Lett. 322*, 56−60.
19. Adam, L. P., Gapinski, C. J., and Hathaway, D. R. (1992) Phosphorylation sequences in h-caldesmon from phorbol ester-stimulated canine aortas, *FEBS Lett. 302*, 223−226.
20. Gerthoffer, W. T., and Pohl, J. (1994) Caldesmon and calponin phosphorylation in regulation of smooth muscle contraction, *Can. J. Physiol. Pharmacol. 72*, 1410−1414.
21. Cook, A. K., Carty, M., Singer, C. A., Yamboliev, I. A., and Gerthoffer, W. T. (2000) Coupling of M(2) muscarinic receptors to ERK MAP kinases and caldesmon phosphorylation in colonic smooth muscle, *Am. J. Physiol. 278*, G429−G437.
22. Gerthoffer, W. T., Yamboliev, I. A., Shearer, M., Pohl, J., Haynes, R., Dang, S., Sato, K., and Sellers, J. R. (1996) Activation of MAP kinases and phosphorylation of caldesmon in canine colonic smooth muscle, *J. Physiol. 495*, 597−609.
23. Nixon, G. F., Iizuka, K., Haystead, C. M. M., Haystead, T. A. J., Somlyo, A. P., and Somlyo, A. V. (1995) Phosphorylation Of Caldesmon By Mitogen-Activated Protein Kinase With No Effect On Ca^{2+} Sensitivity In Rabbit Smooth Muscle, *J. Physiol. 487*, 283−289.
24. Hedges, J. C., Oxhorn, B. C., Carty, M., Adam, L. P., Yamboliev, I. A., and Gerthoffer, W. T. (2000) Phosphorylation of caldesmon by ERK MAP kinases in smooth muscle, *Am. J. Physiol. 278*, C718−C726.
25. Redwood, C. S., Marston, S. B., and Gusev, N. B. (1993) The functional effects of mutations Thr673→Asp and Ser702→Asp at the Pro-directed kinase phosphorylation sites in the C-terminus of chicken gizzard caldesmon, *FEBS Lett. 327*, 85−89.
26. Krymsky, M. A., Chibalina, M. V., Shirinsky, V. P., Marston, S. B., and Vorotnikov, A. V. (1999) Evidence against the regulation of caldesmon inhibitory activity by p42/p44erk mitogen-activated protein kinase in vitro and demonstration of another caldesmon kinase in intact gizzard smooth muscle, *FEBS Lett. 452*, 254−258.
27. Patchell, V. B., Vorotnikov, A. V., Gao, Y., Low, D. G., Evans, J. S., Fattoum, A., El-Mezgueldi, M., Marston, S. B., and Levine, B. A. (2002) Phosphorylation of the minimal inhibitory region at

the C-terminus of caldesmon alters its structural and actin binding properties, *Biochim. Biophys. Acta 1596*, 121−130.
28. Childs, T. J., Watson, M. H., Sanghera, J. S., Campbell, D. L., Pelech, S. L., and Mak, A. S. (1992) Phosphorylation of smooth muscle caldesmon by mitogen-activated protein (MAP) kinase and expression of MAP kinase in differentiated smooth muscle cells, *J. Biol. Chem. 267*, 22853−22859.
29. Guo, H., Bryan, J., and Wang, C.-L. A. (1999) A note on the caldesmon sequence, *J. Muscle Res. Cell Motil. 20*, 725−726.
30. Tao, T., and Lamkin, M. (1981) Excitation energy transfer studies on the proximity between SH1 and the adenosinetriphosphatase site in myosin subfragment 1, *Biochemistry 20*, 5051−5055.
31. Tao, T., Lamkin, M., and Lehrer, S. S. (1983) Excitation energy transfer studies of the proximity between tropomyosin and actin in reconstituted skeletal muscle thin filaments, *Biochemistry 22*, 3059−3066.
32. Tao, T., Gowell, E., Strasburg, G. M., Gergely, J., and Leavis, P. C. (1989) Ca^{2+} dependence of the distance between Cys-98 of troponin C and Cys-133 of troponin I in the ternary troponin complex. Resonance energy transfer measurements, *Biochemistry 28*, 5902−5908.
33. Fairclough, R. H., and Cantor, C. R. (1978) The use of singlet-singlet energy transfer to study macromolecular assemblies, *Methods Enzymol. 48*, 347−379.
34. Stryer, L. (1978) Fluorescence Energy Transfer As a Spectroscopic Ruler, *Annu. Rev. Biochem. 47*, 819−846.
35. Chantler, P. D., and Tao, T. (1986) Interhead fluorescence energy transfer between probes attached to translationally equivalent sites on the regulatory light chains of scallop myosin, *J. Mol. Biol. 192*, 87−99.
36. Chifflet, S., Torriglia, A., Chiesa, R., and Tolosa, S. (1988) A method for the determination of inorganic phosphate in the presence of labile organic phosphate and high concentrations of protein: application to lens ATPases, *Anal. Biochem. 168*, 1−4.
37. Clauser, K. R., Baker, P. R., and Burlingame, A. L. (1999) Role of accurate mass measurement (±10 ppm) in protein identification strategies employing MS or MS/MS and database searching, *Anal. Chem. 71*, 2871−2882.
38. Field, M., Papac, D., and Jones, A. (1996) The use of high-performance anion-exchange chromatography and matrix-assisted laser desorption/ionization time-of-flight mass spectrometry to monitor and identify oligosaccharide degradation, *Anal. Biochem. 239*, 92−98.
39. Berlin, K., Jain, R. K., Tetzlaff, C., Steinbeck, C., and Richert, C. (1997) Spectrometrically monitored selection experiments: quantitative laser desorption mass spectrometry of small chemical libraries, *Chem. Biol. 4*, 63−77.
40. Wang, C.-L. A. (1988) Photocrosslinking of calmodulin and/or actin to chicken gizzard caldesmon, *Biochem. Biophys. Res. Commun. 156*, 1033−1038.
41. Qin, J., and Zhang, X. (2002) Identification of in vivo protein phosphorylation sites with mass spectrometry, *Methods Mol. Biol. 194*, 211−221.
42. D'Angelo, G., Graceffa, P., Wang, C.-L. A., Wrangle, J., and Adam, L. P. (1999) Mammal-specific, ERK-dependent, caldesmon phosphorylation in smooth muscle, *J. Biol. Chem. 274*, 30115−30121.
43. Galazkiewicz, B., Mossakowska, M., Osinska, H., and Dabrowska, R. (1985) Polymerization of G-actin by caldesmon, *FEBS Lett. 184*, 144−149.
44. Makuch, R., Kulikova, N., Graziewicz, M. A., Nowak, E., and Dabrowska, R. (1994) Polymerization of actin induced by actin-binding fragments of caldesmon, *Biochim. Biophys. Acta 1206*, 49−54.
45. Dabrowska, R., Goch, A., Galazkiewicz, B., and Osinska, H. (1985) The influence of caldesmon on ATPase activity of the skeletal muscle actomyosin and bundling of actin filaments, *Biochim. Biophys. Acta 842*, 70−75.
46. Moody, C. J., Marston, S. B., and Smith, C. W. J. (1985) Bundling of actin filaments by aorta caldesmon is not related to its regulatory function, *FEBS Lett. 191*, 107−112.
47. Mornet, D., Harricane, M.-C., and Audemard, E. (1988) A 35-kilodalton fragment from gizzard smooth muscle caldesmon that induces F-actin bundles, *Biochem. Biophys. Res. Commun. 155*, 808−815.
48. Wang, Z., Horiuchi, K. Y., and Chacko, S. (1996) Characterization of the functional domains on the C-terminal region of caldesmon using full-length and mutant caldesmon molecules, *J. Biol. Chem. 271*, 2234−2242.
49. Gao, Y., et al. (1999) The interface between caldesmon domain 4b and subdomain 1 of actin studied by nuclear magnetic resonance spectroscopy, *Biochemistry 38*, 15459−15469.
50. Zhuang, S., Wang, E., and Wang, C.-L. A. (1995) Identification of the functionally relevant calmodulin binding site in smooth muscle caldesmon, *J. Biol. Chem. 270*, 19964−19968.
51. Wang, Z., Yang, Z. Q., and Chacko, S. (1997) Functional and structural relationship between the calmodulin-binding, actin-binding, and actomyosin-ATPase inhibitory domains on the C terminus of smooth muscle caldesmon, *J. Biol. Chem. 272*, 16896−16903.
52. Huber, P. A. J., Gao, Y., Fraser, I. D. C., Copeland, O., El-Mezgueldi, M., Slatter, D. A., Keane, N. E., Marston, S. B., and Levine, B. A. (1998) Structure−activity studies of the regulatory interaction of the 10 kilodalton C-terminal fragment of caldesmon with actin and the effect of mutation of caldesmon residues 691−696, *Biochemistry 37*, 2314−2326.
53. Sobue, K., Muramoto, Y., Fujita, M., and Kakiuchi, S. (1981) Purification of a calmodulin-binding protein from chicken gizzard that interacts with F-actin, *Proc. Natl. Acad. Sci. U.S.A. 78*, 5652−5655.
54. Pinter, K., and Marston, S. B. (1992) Phosphorylation of vascular smooth muscle caldesmon by endogenous kinase, *FEBS Lett. 305*, 192−196.
55. Humphrey, M. B., Herrera-Sosa, H., Gonzalez, G., Lee, R., and Bryan, J. (1992) Cloning of cDNAs encoding human caldesmons, *Gene 112*, 197−204.
56. Goncharova, E. A., Vorotnikov, A. V., Gracheva, E. O., Wang, C.-L. A., Panettieri, R. A., Jr., Stepanova, V. V., and Tkachuk, V. A. (2002) Activation of p38 MAP-kinase and caldesmon phosphorylation are essential for urokinase-induced human smooth muscle cell migration, *Biol. Chem. 383*, 115−126.
57. Yamashiro, S., Yamakita, Y., Yoshida, K., Takiguchi, K., and Matsumura, F. (1995) Characterization of the COOH terminus of non-muscle caldesmon mutants lacking mitosis-specific phosphorylation sites, *J. Biol. Chem. 270*, 4023−4030.

BI0268605